An Inexpensive Chest Belt for measuring Respiratory Effort

Maximilian Geiger, Philipp Fleck, and Clemens Arth

***Abstract*— Sleep significantly affects health and well-being, but sleep apnea and other breathing problems remain critical problems. Polysomnography (PSG), the standard diagnostic method, is often costly and uncomfortable and is performed in specialized sleep laboratories. The respiratory-induced plethysmography sensor, the benchmark for measuring respiratory effort in sleep diagnosis, is expensive, prompting the need for cheaper alternatives.**

This project aims to develop an affordable chest strap that uses a strain gauge to measure chest expansion for breathing effort. The goal is to integrate this technology into a home PSG device to detect sleep apnea comfortably. The sleeping position is also monitored for its potential impact on apnea. This chest strap records respiratory activity during sleep, with data processed for analysis to offer an effective alternative to traditional sleep diagnostics.

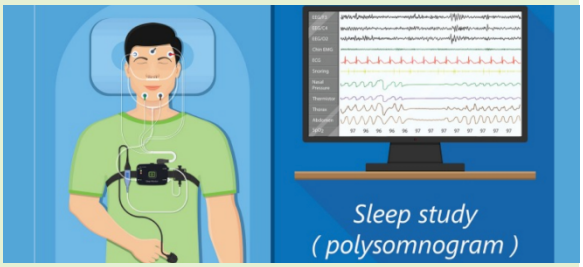

***Index Terms*— respiratory effort, biological signals, sleeping position, chest belt.**

I. Introduction

Sleep is a fundamental aspect of life and therefore exerts a substantial influence on the health and well-being of individuals. However, it is important to note that complications and illnesses that affect respiratory function can also arise in connection with sleep. In the contemporary era, it is becoming increasingly necessary to diagnose these problems. Currently, there is an increasing focus on improving patient comfort, with the aim of avoiding substantial costs.

Sleep apnea is a common disease[1], around 6% in the US alone. The standard diagnostic procedure for this condition is PSG. This procedure is performed in a specialized sleep laboratory, an environment in which the subject is likely unfamiliar. The respiratory aspect of sleep is a crucial biofactor in the diagnostic process. Specifically, respiratory effort plays an important role in the diagnostic process. The gold standard for recording respiratory effort is the respiratory-induced plethysmography (RIP) sensor. Consequently, it is a highly effective variant, although it is also very expensive. Given that the RIP procedure involves the measurement of rib cage expansion, it is logical to utilize strain gauges for this purpose. In addition, such a chest strap can be used to establish additional respiratory parameters, including respiratory rate and respiratory depth.

Our goal is to design an economical chest belt to measure chest movement, a derivative of respiratory effort, with wireless data transmission for easy integration into various systems. The aim is to integrate this belt into a domestic PSG system with sensors to facilitate sleep apnea detection. By minimizing costs, individuals can conduct PSG at home. Movement measurement is achieved using a strain gage on an elastic belt, ensuring data comparable to that of a RIP sensor.

Our goal for now is **not** to create a clinical device, but to show the serious potential of commodity hardware for mainly educational and private purposes. Although a clinical study would give further and more sophisticated insights, this task lies outside the scope of our current work, requiring significant effort and administration which is unmanageable for the time being. However, in the latter part of this work we still compare our prototype to a gold standard device to proof the potential of our solution.

Another significant factor that has the ability to exacerbate or mitigate sleep apnea is sleep posture. Although it is not a significant indicator in terms of facilitating diagnosis, it is nonetheless interesting to observe the correlation between the data and the breathing data, as well as the dependence of rib cage expansion on the sleeping position. Observing sleeping posture and its integration into the prevailing thoracic configuration is a straightforward process. A 3-axis gyroscope

"The VRVis GmbH is funded by BMK, BMAW, Tyrol, and Vienna Business Agency in the scope of COMET - Competence Centers for Excellent Technologies (911654) which is managed by FFG. Funded by the European Union under Grant Agreement No. 101092861. Views and opinions expressed are, however, those of the author(s) only and do not necessarily reflect those of the European Union or the European Commission. Neither the European Union nor the granting authority can be held responsible for them."

M. Geiger is a student of Computer Science at Graz University of Technology, AT (e-mail: maximilian.geiger@student.tugraz.at).

P. Fleck is a senior scientist, formerly with Graz University of Technology, AT, and now at VRVis GmbH, Vienna, AT (e-mail: philipp.fleck@tugraz.at).

C. Arth is a senior scientist at Graz University of Technology, AT (e-mail: clemens.arth@tugraz.at).

[1] https://pmc.ncbi.nlm.nih.gov/articles/PMC4561280/

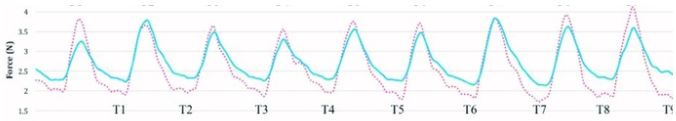

Fig. 1: Breathing: measured with a chest strap (dotted red) and with an abdominal belt (solid red) over time as shown by Bai *et al*. [8].

and 3-axis accelerometer are used to assess sleep in four distinct positions.

Another objective is to monitor respiratory parameters during diurnal activities. By comparing these recorded data, it may be possible to draw conclusions about exertion, stress, or similar. Ultimately, the final data are to be presented and prepared for evaluation.

II. Related Work

We briefly describe the process of polysomnography and to highlight which aspects of breathing are of particular significance and can be quantified with the use of a chest belt.

PSG is a diagnostic procedure that enables the objective assessment of sleep and sleep associated disorders. According to Markun *et al*. [1]. PSG records multiple physiological activities during sleep and is the gold standard for sleep studies and diagnosing sleep disorders, especially those related to breathing. It is crucial when medical history alone is insufficient for diagnosis.

Certain components are crucial in recognizing that sleep disorders are related to breathing, such as respiratory flow, effort, rate, depth, and pattern, as noted by Martinot *et al*. [2]. The assessment of respiratory effort is particularly vital, as highlighted by Park *et al*. [3].

According to Vandenbussche *et al*. [4], the standard PSG setup uses two belts. A chest strap alone may suffice for monitoring respiratory rate or in thoracic-breathing patients. For sleep-related breathing disorders, using a chest strap alone or combined with an abdominal strap is crucial due to complex sleep breathing patterns, especially in obstructive sleep apnea (OSA). Monitoring respiratory efforts is essential to distinguish between obstructive sleep apnea (OSA) and central sleep apnea (CSA). A chest strap using respiratory-induced plethysmography (RIP) offers a non-invasive way to measure respiratory effort, which involves the necessary muscular activity for breathing [4]. The gold standard [5], for measuring respiratory effort non-invasively is the RIP. According to the definition of the American Academy of Sleep Medicine (AASM), an apnea lasts at least 10 seconds [6].

Landry *et al*. [7] extensively researched the link between sleep position and obstructive sleep apnea (OSA). Thus, it's crucial to consider the patient's usual sleep position when interpreting PSG results. Our protype can distinguish between sleep positions, while monitory the chest cage expansion.

A. Sensors and Methods

Vandenbussche *et al*. [4] demonstrate how to measure effort, rate, depth, and pattern with non-invasive approaches. Zhang *et al*. [9] describes the RIP system using two belts on the thorax and abdomen to measure inductance changes caused by breathing. High-frequency current flows through coils in the belts, altering inductance as the patient breathes.

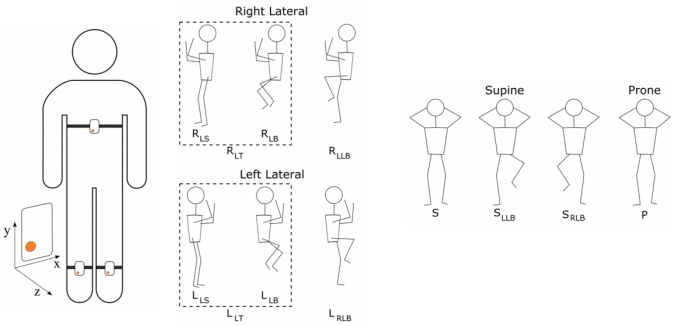

Fig. 2: Different sleeping positions differentiated in the study [16] and their categorisation using three Sensors.

Park *et al*. [2] show that RIP sensor data correlates highly with standard PSG sensors but underestimates some events compared to nasal sensors. Polyvinylidene fluoride (PVDF) sensors serve as an alternative [10] to RIP sensors due to their piezoelectric properties, generating electrical signals when deformed.

Koo *et al*. [6] gives detailed insights into the comparison between the PVDF impedance belt (PVDFb) and RIP for measuring respiratory events during PSG. They demonstrate that PVDFb exhibits comparable event detection accuracy, good signal quality, and high reliability. The configuration of how a respiratory recording using a chest strap should look like is illustrated in Figure 1.

An alternative method, shown by Kristiansen *et al*. [11] uses strain gauges [12] to measure the change of the rib cage. Liu *et al*. [13] examined the validity and reliability of a recently developed wearable strain sensor (WSS) for the purpose of measuring respiratory movements. Acquiring values from strain gauges on skin is a multi-step procedure as demonstrated by Langon *et al*. [14]. In order to directly determine the expansion of biological material such as the skin, a number of different types of strain gauges are described by Lu *et al*. [15]. One potential method of detecting sleeping positions is to utilise an accelerometer. Fallmann *et al*. [16] use a three 3-axis accelerometers integrated into three Shimmer3devices were utilised to determine the subject's sleeping position. The employment of three sensors facilitates the detection of relevant lower limb movements, thereby enabling the recognition of positions with greater granularity (Figure 2).

Dohen *et al*. [17] described a method using a three-axis accelerometer on the upper body to detect sleep positions, which inspired us to use a similar categorization in our prototype.

B. Software

Bluetooth Low Energy (BLE) is an emerging low-power wireless technology that has found application in a variety of contexts [18] such as home appliances and wearables. The BLE system utilises a connection event structure, whereby devices exchange data at regular intervals. Each connection

TABLE I: Cost Estimate of Commercial Products

Vendor	Product	Price (USD)
Venier [19]	Go Direct® Respiration Belt	150-300
Perfect Fit [20]	PVDF Effort Belt Kits	350-950
Natus® [21]	RIP Respiratory Effort Belts	1100-1200
Ours	ESP, Strain Gauge, MPU, ...	< 30

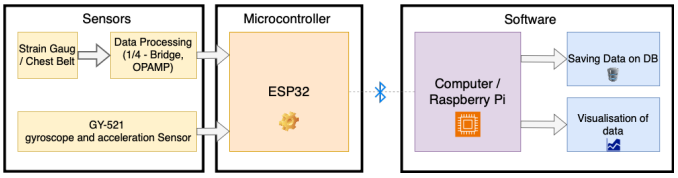

Fig. 3: Component interplay of our prototype, divided into three parts: Senors (yellow), Microcontroller (orange), Software (purple and blue).

event can contain multiple send and receive events to transmit data packets.

The data concerning the act of respiration is principally represented as amplitude curves over time [6], [10]. Furthermore, selecting an appropriate sampling rate is essential for effective capture of the pertinent information within the respiratory signal. When recording the signals with the strain gauge sensor, a sampling rate of 10 Hz is applied to the respiratory data [11] and is downsampled to 1 Hz for analysis.

C. Commercial Products

In Table I a number of commercial products to capture breathing patterns are listed. Because availability and prices vary drastically, only a price range is given, in addition to the estimated cost for components to build our belt. Arguably the cost of our prototype is considerably cheaper than any commercial product.

III. Prototype Development

In this section we will go through the individual conceptual components of our prototype. In a nutshell, the data from the measurements of breast movement and sleeping position are recorded and sent to a data recorder which processes, stores the data and prepares the visualizations.

The key function of the sensor in measuring chest movement is detecting ribcage expansion and converting it into a signal. Most sensors require a measurement processing unit with a measuring bridge and amplifier after the sensor. The assertion is made that a standard amplifier for bridge circuits is a subtraction amplifier [22]. The general calculation for the Output voltage is given in Equation 1, where the variables denote resistores (R_n) and voltages (U_x) in the schematic (Figure 5).

$$U_a = -\left(\frac{R_5}{R_4}\right)(U_{e2} - U_{e1}) \tag{1}$$

The sleep position detection sensor identifies body positions and provides distinguishing data. Sensors attached to the sleeper, particularly accelerometers, capture body movements and orientation changes, allowing calculations of roll and pitch.

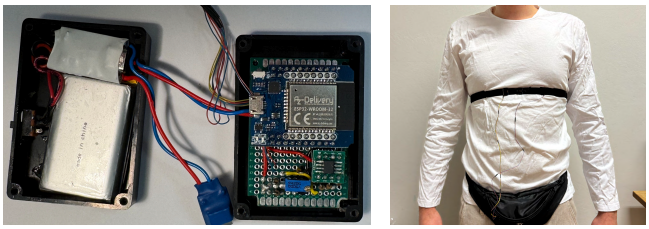

Fig. 4: The ESP32 and the battery (left) are connected to the belt (right) together with the strain gauge and the accelerometer.

$$\text{Pitch} = \theta = \arcsin\frac{a_x}{g} = \arcsin\frac{a_x}{\sqrt{a_x^2 + a_y^2 + a_z^2}} \tag{2}$$

$$\text{Roll} = \phi = \arctan\frac{a_y}{a_z} \tag{3}$$

Wrona [23] show in Equation 2 and Equation 3 how to compute pitch and roll, where a_x, a_y, a_z represent the acceleration components along the respective axes of a Cartesian coordinate system and $g \approx 9.81 m/s^2$ the gravitational force. These values are typically obtained from an acceleration sensor (accelerometer). The axes are aligned so that they are defined in relation to the object of the sensor. The x-axis is defined as forwards/backwards, the y-axis as sideways or left/right and the z-axis as up/down.

It is possible to categorize five different body positions during sleep using roll and pitch. Specifically, these positions include: i) sleeping on the right side, ii) sleeping on the left side, iii) lying on the back, iv) lying on the belly, and v) other positions that involve sitting up or between positions. The following categorizations in Table II can be deduced from the extant literature by Tawil *et al.* [24] and Torres *et al.* [25] and the fundamental principles of roll and pitch. In our practical implementation, as depicted in Figure 3, the system is divided into two parts.

- a wearable data recording setup, containing the belt, the strain gauge and the accelerometer, controlled by an ESP32; and
- an accompanying Raspberry Pi, which serves as a data receiver, storage and visualization device.

For the strain gauge to work properly, we concentrate the elasticity in one specific spot of the belt and keep most of the circumference rigid. The accelerometer is also mounted on the belt itself. The enclosure contains the ESP32 and the battery and is connected by cable (see Figure 4). The strain gauge is integrated into a quarter bridge configuration [14] for high sensitivity and uses the full ADC range of the ESP32. A Wheatstone bridge circuit and a spindle potentiometer ensure balance and optimal sensitivity [22]. The ESP32 measures the value at the ADC once every 100 milliseconds. To facilitate the recording of all values, the acceleration values are also recorded at the same rate. In addition, the values are transmitted to the terminal device at an interval of 100 ms. Data are transmitted using BLE, which offers advantages in power consumption over WiFi for our use case, as shown in Table III.

As illustrated in Figure 5, the bridge voltage is amplified using a subtraction amplifier. The gain is approximately 1000, which ensures that the range of the ADC is well utilised.

TABLE II: Sleeping positions in relation to roll and pitch, with its optimal values.

Sleeping Position	Roll [°]	Pitch [°]
right side	-90	-180
left side	90	180
back	0	0
belly	0	±180

TABLE III: Belt power consumption for transmission protocols.

Transmission	CPU[MHz]	Consumption [mA]
Wi-Fi	240	110
BLE	240	70
BLE	80	50

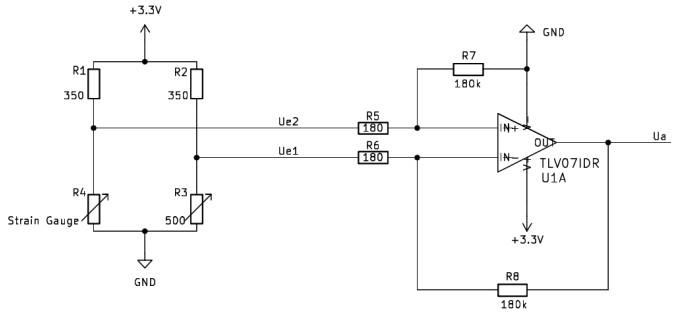

Fig. 5: Schematics of the quarter bridge and the amplifier circuit.

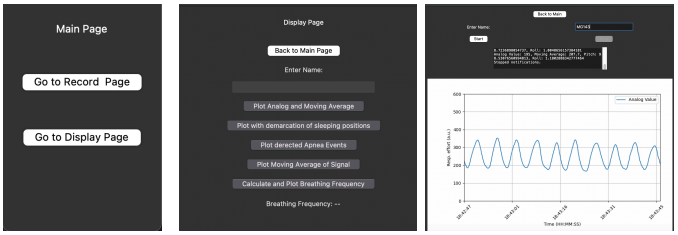

Fig. 6: GUI: (left) shows the main page, (middle) shows the display page, and (right) shows the record page.

The amplification was calculated as follows. By measuring the bridge voltage, it was determined that the maximum change in the bridge voltage is between 2-3 mV. To utilise the full 3.3 V ADC input voltage of the ESP32 results in an amplification of 1000.

We use a Raspberry Pi as the BLE endpoint to store (SQLite) recorded data, to run the user interface (see Figure 6) and to create visualizations. Roll and Pitch are utilized to display the sleeping positions, which are categorized using simple if-else statements. Subsequently, the sleeping positions are displayed using a color-coding system, in which the background of the breathing pattern is rendered according to the specific sleeping position. The incoming signal from the strain gauge is filtered with a moving average filter (see Figure 7) with an adjustable window size to reduce noise. For all recordings presented in this paper, we applied a moving average window of 15 samples, where each output value represents the arithmetic mean of the most recent 15 data points. Based on the filtered data, we create a visualization (see Figure 8) of breathing patterns and corresponding sleep positions.

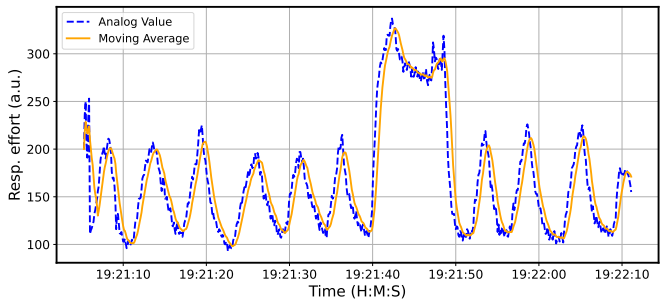

Fig. 7: Raw data (blue) compared to filtered data (red) using an moving average with adaptive window.

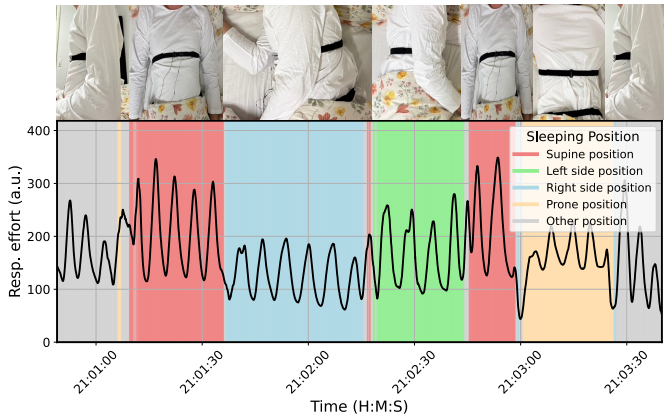

Fig. 8: Simulated breathing pattern such as changing sleeping positions, color mapped to indivudal states.

The data can be visualized in two ways: real-time, like an ECG monitor, or as a complete recording to analyze breathing patterns. The UI supports live-data viewing and stored data analysis. Data can be named, added, and deleted. The algorithm calculates respiratory rate by converting timestamps to relative seconds, identifying and filtering signal peaks, verifying dips between peaks, and calculating time intervals to determine the average rate in breaths per minute.

IV. Evaluation

In the following, we discuss the data acquired with the belt prototype and analyze several recordings. In addition, we examine the limitations of our prototype. The interested reader is referred to the work of Geiger [26] for more details.

A. Self-tests

All recordings were conducted in self-tests and the same belt was utilized for all recordings. This was positioned at the same level as the ribcage throughout the testing process.

One potential application of the belt is to detect events of apnea. This is achieved by holding air in the lungs after exhalation. Figure 9 shows, that our belt is capable of detecting events like respiratory arrest when breathing stops. This phenomenon can be discerned by the absence of respiratory movement, which results in the formation of a straight line at the values resp. effort 120.

Figure 10 shows a simulated recording of respiratory effort, which was obtained while the subject was sitting and not in a

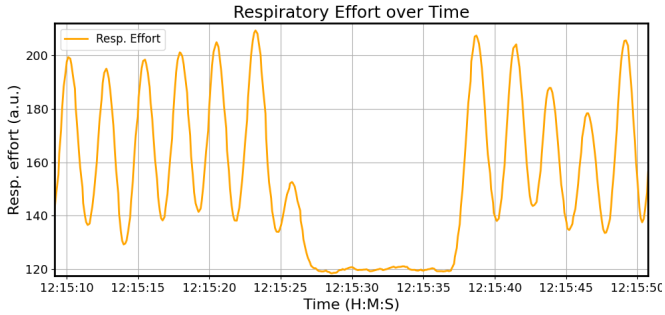

Fig. 9: Simulated breathing pattern that incorporates a pause in breathing. During this pause, the subject is instructed to hold their breath.

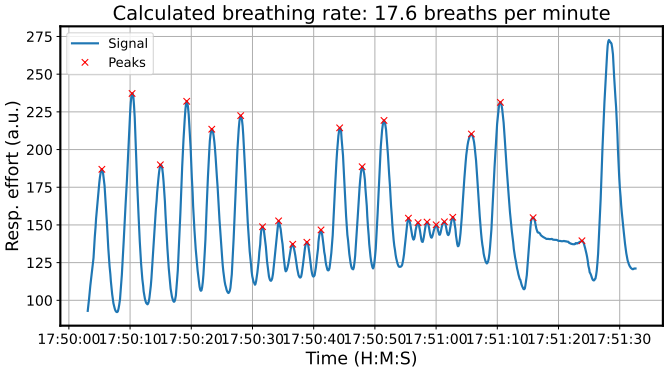

Fig. 10: Recording to determine the respiratory rate. The respiratory peaks are marked in red.

state of sleep. The breathing frequency of the recorded signal is 17.6 *breaths per minute*. In addition, the respiratory peaks utilized for the calculation of the respiratory frequency are indicated in red.

The left of Figure 11 shows the respiratory effort during a long period of sleep. The background is colored according to the sleeping position. It is evident that the measurement data exhibit a high level of variability during positional transitions, yet the measurement remains operational within the defined positions. In addition, the initial area demonstrates the phase of falling asleep (first 20 minutes), during which the respiratory effort exhibits an increase relative to the rest of the sleep. The right of Figure 11 illustrates the filtered image of the respiratory effort, showing a small portion of the same recording. The respiratory effort is indicated by the orange line, which is mapped over a period of one minute and 30 seconds.

The top of Figure 12 shows data containing multiple sneezes. It is evident that the implementation of a moving average filter significantly attenuates the peaks associated with these events, resulting in a more uniform distribution. The instances of sneezing are denoted by red boxes. It is important to note that the act of sneezing was challenging to record in reality, and therefore the subject was replicated during the recording process.

In analogy, the bottom of Figure 12 shows the recording of multiple coughs. The application of a moving average filter significantly reduces the presence of cough-related spikes in the data. Consequently, coughs are more easily discernible in

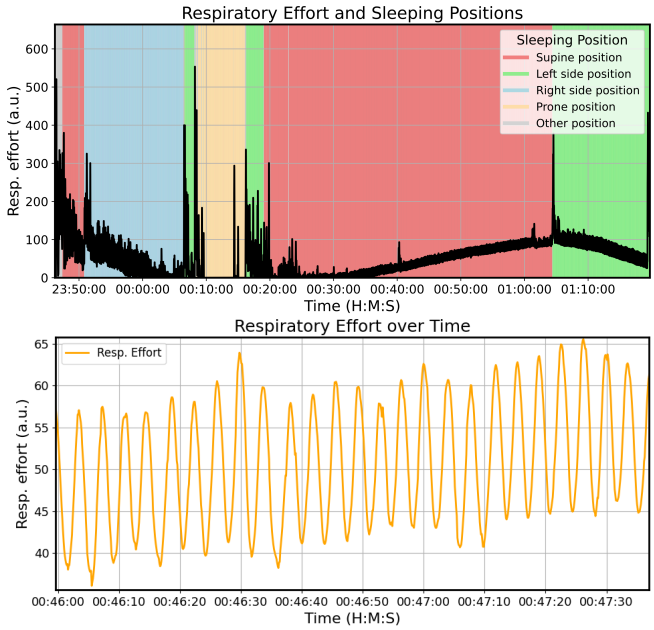

Fig. 11: (Top) shows the nocturnal respiratory activity, encompassing the entirety of a night's sleep. (Bottom) shows 1m30sec starting 46 min after midnight.

TABLE IV: Overview of the three measurement blocks, including belt type, belt positions, and number of recordings.

Testname	Belt	Belt positions	Recordings
Ultra baseline load test	ESP	fixed (weight test)	15
	Vernier	fixed (weight test)	15
Static baseline breathing	ESP	3 upper / 3 lower	6
	Vernier	3 lower / 3 upper	6
Dynamic breathing test	ESP	alternating	4
	Vernier	alternating	4

unfiltered data (*i.e.* the original data) compared to filtered data. The cough events are marked by red boxes.

B. Comparison

To validate the reliability of the self-developed respiration belt, measurements were compared with the Vernier Go Direct® Respiration Belt (in the following referred to as *Vernier belt*), a widely used experimental reference system. As stated in the dissertation by Mahdi [27], the device is frequently used as a benchmark in studies involving respiratory monitoring technologies. Another justification for selecting this belt is provided by Hayward *et al*. [28], who highlight that the sensor produces a strong respiration signal with no detectable artifacts in the raw data. They emphasize that the belt offers a non-invasive and direct measurement of thoracic expansion, which is considered equivalent to manual chest movement counts. In addition, Ross *et al*. [29] describe the *Vernier belt* as a robust physiological measurement tool capable of accurately establishing the ground-truth respiratory rate for comparison against novel sensing technologies. Additional evidence comes from the Binah.ai SDK Accuracy Study [30], in which the *Vernier belt* served as an approved reference device along with a certified Masimo finger pulse oximeter, which is a gold standard for measuring brpm. In this large-scale evaluation, the

This article has been accepted for publication in IEEE Sensors Journal. This is the author's version which has not been fully edited and
content may change prior to final publication. Citation information: DOI 10.1109/JSEN.2026.3668016

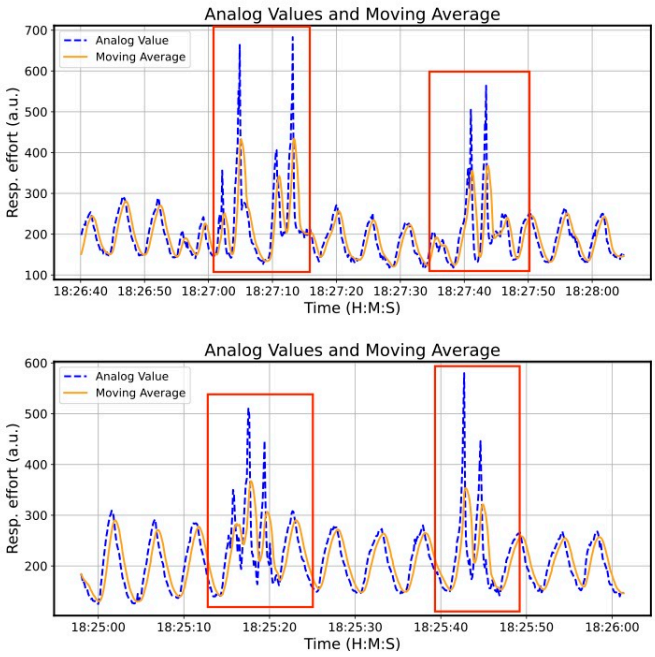

Fig. 12: Top: **Sneeze detection** - raw and the filtered data of a test signal in which sneezing occurred twice. The sneezing events are outlined with the red boxes. Bottom: **Cough detection** - raw data and filtered data of a test signal in which two coughs were made. The coughing events are outlined with red boxes.

belt provided the ground truth of respiratory-rate to validate a remote photoplethysmography algorithm across diverse populations and conditions in multiple countries, including Israel, India, South Africa and Japan.

Hayward *et al*. [28] also used the belt as a comparator strain-gage chest monitor in their evaluation of a novel capacitive-based respiration sensor. It recorded the expansion force of the chest during controlled metronome-paced breathing and resting conditions in healthy volunteers, serving as a reliable reference signal. Similarly, Ross *et al*. [29] used the *Vernier belt* as a wired respiration measurement device to establish ground truth for comparison with a wireless Bellyband sensor. By synchronizing both systems through predefined deep-breath maneuvers, the study quantified bias and RMSE in a wide range of respiratory-rates (10 to 70 breaths per minute), once again demonstrating the suitability of the *Vernier belt* for accurate reference measurements.

Together, these studies demonstrate that the *Vernier belt* consistently provides a stable, artifact-free, and physiologically meaningful measurement of chest expansion, which makes it suitable to serve as a baseline reference device in experimental respiration research.

1) Weight Test: In order to demonstrate the reliability of the self-built belt compared to the established *Vernier belt*, an ultra baseline load test was conducted. This test was used to compare the mechanical response of the custom-built respiratory belt with that of the *Vernier belt* under controlled static loading. One end of each belt was fixed while calibrated masses were attached to the free end, starting with 200 g and followed by two increments of 50 g (resulting in 200 g, 250 g, and 300 g load conditions). The mounting setup is shown on the left of Figure 13, while the testing conditions are listed in Table IV.

Fig. 13: Left: the setup of the ultra baseline load test. Right: two thoracic mounting positions of the respiratory belts.

For each load step, five repeated measurements were recorded for both belts. The resulting datasets, presented in Figure 14, include raw and moving-average–filtered signals. The moving average filter was again set up with a window size of 15. Across all measurements, both systems show a clear reduction in signal variability when comparing raw data with moving-average-filtered curves. The ESP belt exhibits more short-term fluctuations in the raw signals, while the moving-average traces form smooth and stable plateaus at each load level. In contrast, the *Vernier belt* shows inherently lower noise and very consistent signal behavior, with its moving-average curves nearly overlapping across repetitions.

When comparing both belts, *Vernier belt* shows tighter clustering and lower baseline noise, while the ESP belt shows slightly greater variation between and within trials. Nevertheless, both systems reliably capture the expected stepwise increase in tension for all load conditions, and moving-average filtering greatly reduces the differences between them.

A small amount of transient noise occurs when additional weights are applied, caused by brief, unavoidable oscillations of the belt. These disturbances are short-lived and do not affect the overall baseline assessment once the system stabilizes.

2) Baseline Tests: Following the observation that the static weight test yielded favorable results, a more active baseline test was conducted. This baseline test comprised six measurements, each with a duration of approximately 15 minutes, which were recorded with the subject in a supine position while breathing naturally. Both respiratory belts were worn concurrently, with their positions alternated between sessions. The two positions where the belts were changed are shown on the right of Figure 13. This ensured that each belt was mounted three times in the lower position and three times in the upper position. The results of the baseline tests are shown in Figure 15.

To facilitate comparison, the correlation of the z-normalized signals was calculated and the breaths per minute (brpm) were determined for both devices. For both belts, a moving-average filter with a window size of 15 was applied. The brpm values were obtained by detecting the peaks in each signal using the same peak-detection algorithm.

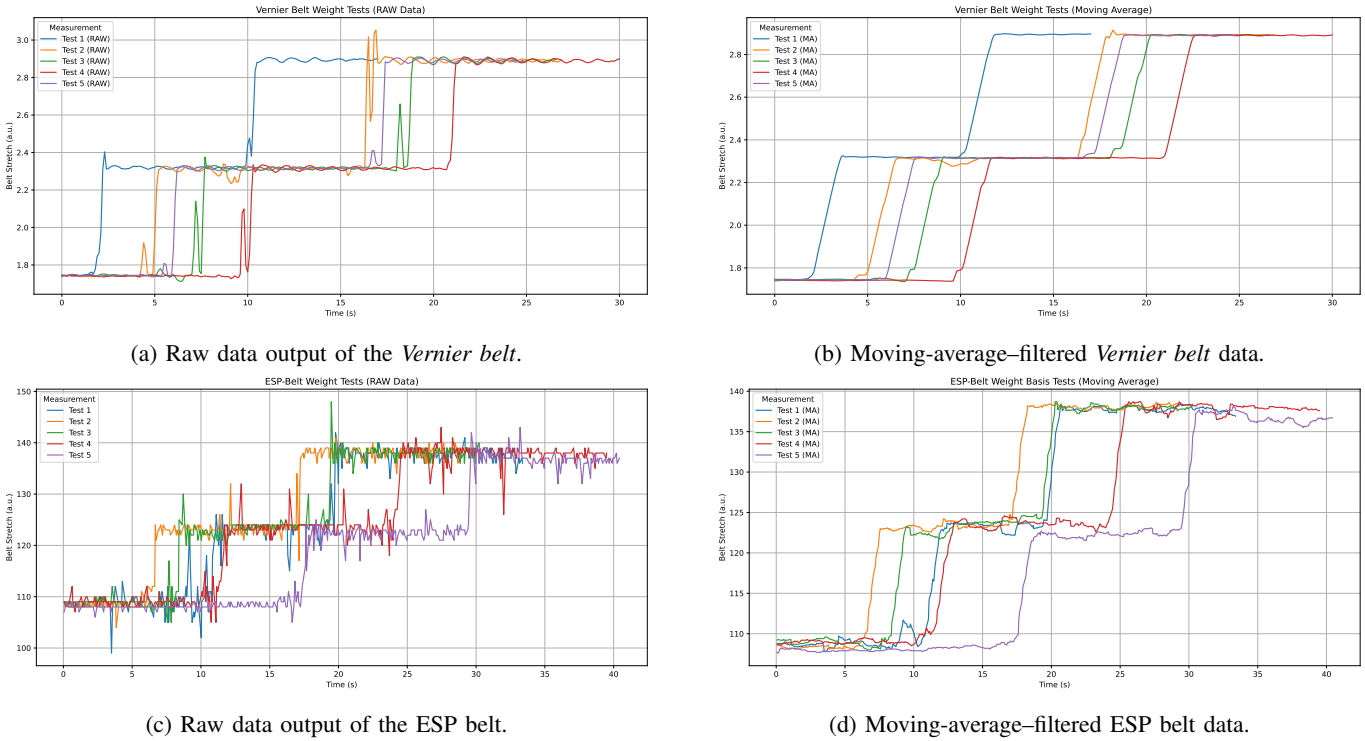

(a) Raw data output of the *Vernier belt*.

(b) Moving-average–filtered *Vernier belt* data.

(c) Raw data output of the ESP belt.

(d) Moving-average–filtered ESP belt data.

Fig. 14: Comparison of raw and moving-average–filtered signals from the *Vernier belt* (top row) and the custom-built ESP belt (bottom row) during the static weight test. Starting with 200 g and followed by two increments of 50 g (resulting in 200 g, 250 g, and 300 g load conditions)

Across all six tests shown in Figure 15, the correlation between the self-assembled belt and the *Vernier belt* exceeds 0.92, and the calculated brpm are essentially identical across all recordings.

3) Respiratory Conditions: After completion of the more active baseline test, a third test block was conducted. As depicted in Figure 16, four dynamic breathing trials were performed within this block to evaluate the performance of both belts under varying respiratory conditions. Each trial adhered to the same protocol: The sequence of breathing techniques involved in this experiment consists of 30 seconds of normal breathing, followed by 30 seconds of deep breathing, then 30 seconds of shallow and fast breathing, and finally 30 seconds of breath-holding. The experiment ends with a final phase of 30 seconds of normal breathing. As in the previous study, both belts were worn simultaneously and their positions were alternated between trials. The correlation between the signals was once more calculated using the z-normalized data.

As the rapid and shallow breathing component would be diminished by the moving-average filter, the signals displayed in Figure 16 represent the raw unfiltered data recorded of both belts. In all four tests, the correlation coefficient exceeds 0.90. A visual inspection of the signal traces further confirms that both belts capture highly similar waveform characteristics.

Throughout the set of recordings, both belts consistently produced essentially the same signal patterns. It should also be noted that the belt position does not exert a substantial influence on the outcome of the measurement. This phenomenon is evident when comparing the corresponding tests in the reference section, specifically in Figure 15 and Figure 16, where the belt positions have been reversed. The integrated test design facilitates a comprehensive comparison across resting and variable breathing patterns, allowing an assessment of waveform similarity, breath cycle detection, and respiratory rate accuracy that remains largely independent of belt placement.

V. Conclusions

In this work, we describe the design and development of a cost-effective belt to measure sleeping positions and respiratory effort. We outline the technical basics and provide some examples of breathing patterns and sleeping positions. The functionality of the prototypical implementation was verified to work very well when comparing the results to the Vernier Go Direct® Respiration Belt. Moreover, the algorithm developed to detect certain events has shown to work also on the *Vernier belt*, despite targeting our own developed belt.

Several improvements are left as future work. Based on the subjects impression, the belt is more comfortable than the Venier belt, owing to its design which is overall more lightweight. To *further* reduce size, the entire measurement set-up could be converted to a small PCB to attach directly to the belt. By miniaturization, it is also possible to integrate a second belt, which is then attached to the abdomen. The configuration of the chest strap can be utilized, with an additional analog input of the ESP32 incorporated. The employment of dual belts facilitates the detection of OSA.

In order to reduce motion artifacts and to mitigate calibration drift, additional features need to be developed, eventually

This article has been accepted for publication in IEEE Sensors Journal. This is the author's version which has not been fully edited and
content may change prior to final publication. Citation information: DOI 10.1109/JSEN.2026.3668016

(a) Test 1: corr. = 0.9774, ESP = 7.53 brpm, Vernier = 7.47 brpm

(b) Test 2: corr. = 0.9448, ESP = 7.78 brpm, Vernier = 7.78 brpm

(c) Test 3: corr. = 0.9218, ESP = 9.11 brpm, Vernier = 9.06 brpm

(d) Test 4: corr. = 0.9525, ESP = 10.3 brpm, Vernier = 9.76 brpm

(e) Test 5: corr. = 0.9669, ESP = 8.35 brpm, Vernier = 8.29 brpm

(f) Test 6: corr. = 0.9507, ESP = 10.03 brpm, Vernier = 9.70 brpm

Fig. 15: Overview of all six basis respiratory belt tests. Across the six trials, the positions of the Vernier belt and the ESP belt were alternated between the upper and lower chest. The plots are numbered Test 1 to Test 6 according to the order in which the measurements were performed.

using machine learning. In order to properly develop such mechanisms, a larger database of annotated recordings is required. This is considered the output of a clinical trial.

REFERENCES

[1] L. C. Markun and A. Sampat, "Clinician-Focused Overview and Developments in Polysomnography," *Current Sleep Medicine Reports*, vol. 6, no. 4, pp. 309–321, Dec. 2020. 2

[2] D.-Y. Park, T. Kim, J. J. Lee, J. H. Ha, and H. J. Kim, "Validity analysis of respiratory events of polysomnography using a plethysmography chest and abdominal belt," *Sleep and Breathing*, vol. 24, no. 1, pp. 127–134, Mar. 2020. 2

[3] J.-B. Martinot, N.-N. Le-Dong, A. Malhotra, and J.-L. Pépin, "Respiratory effort during sleep and prevalent hypertension in obstructive sleep apnoea," *The European Respiratory Journal*, vol. 61, no. 3, p. 2201486, Mar. 2023. 2

[4] N. L. Vandenbussche, S. Overeem, J. P. Van Dijk, P. J. Simons, and D. A. Pevernagie, "Assessment of respiratory effort during sleep: Esophageal pressure versus noninvasive monitoring techniques," *Sleep Medicine Reviews*, vol. 24, pp. 28–36, Dec. 2015. 2

[5] F. Schipper, R. Jg Van Sloun, A. Grassi, S. Overeem, and P. Fonseca, "A deep-learning approach to assess respiratory effort with a chest-worn accelerometer during sleep," *Biomedical Signal Processing and Control*, vol. 83, p. 104726, May 2023. 2

[6] B. B. Koo, C. Drummond, S. Surovec, N. Johnson, S. A. Marvin, and S. Redline, "Validation of a Polyvinylidene Fluoride Impedance Sensor for Respiratory Event Classification during Polysomnography," *J. of Clinical Sleep Medicine*, vol. 07, no. 05, pp. 479–485, Oct. 2011. 2, 3

[7] S. A. Landry, C. Beatty, L. D. Thomson, A.-M. Wong, B. A. Edwards, G. S. Hamilton, and S. A. Joosten, "A review of supine position related obstructive sleep apnea: Classification, epidemiology, pathogenesis and treatment," *Sleep Medicine Reviews*, vol. 72, p. 101847, Dec. 2023. 2

[8] Z.-M. Bai, Y.-T. Sun, W.-M. Liang, I. Truskauskaitė, M.-E. Yan, C.-R. Li, J. Xiao, M. Aihemaiti, L. Yuan, and O. Rukšėnas, "Respiratory Movements at Different Ages," *Medicina*, vol. 59, no. 6, p. 1024, May 2023. 2

[9] Z. Zhang, J. Zheng, H. Wu, W. Wang, B. Wang, and H. Liu, "Development of a Respiratory Inductive Plethysmography Module Supporting Multiple Sensors for Wearable Systems," *Sensors*, vol. 12, no. 10, pp. 13 167–13 184, Sep. 2012. 2

[10] Y.-Y. Chiu, W.-Y. Lin, H.-Y. Wang, S.-B. Huang, and M.-H. Wu, "Development of a piezoelectric polyvinylidene fluoride (PVDF) polymer-based sensor patch for simultaneous heartbeat and respiration monitoring," *Sensors and Actuators A: Physical*, vol. 189, pp. 328–334, Jan. 2013. 2, 3

[11] S. Kristiansen, K. Nikolaidis, T. Plagemann, V. Goebel, G. M. Traaen, B. Øverland, L. Akerøy, T.-E. Hunt, J. P. Loennechen, S. L. Steinshamn, C. H. Bendz, O.-G. Anfinsen, L. Gullestad, and H. Akre, "A clinical evaluation of a low-cost strain gauge respiration belt and machine

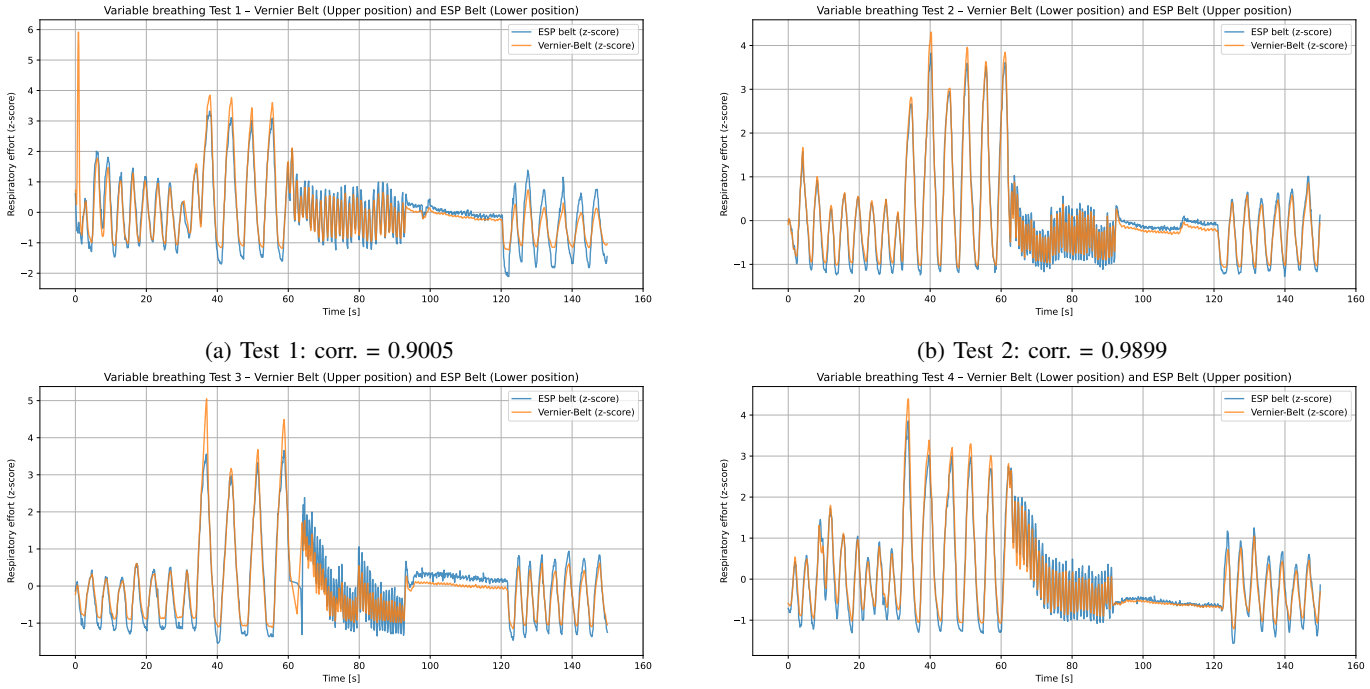

(a) Test 1: corr. = 0.9005

(b) Test 2: corr. = 0.9899

(c) Test 3: corr. = 0.9296

(d) Test 4: corr. = 0.9820

Fig. 16: Overview of all four variable-breathing respiratory belt tests. The figure shows four trials in which the positions of the Vernier belt and the ESP belt were alternated between the upper and lower thorax, with the subplots numbered according to the chronological order of the measurements. Each variable-breathing trial consists of 30s of normal breathing, 30s of deep breathing, 30s of shallow fast breathing, 30s of breath-holding, and a final phase of 30s of normal breathing.

learning to detect sleep apnea," *Smart Health*, vol. 27, p. 100373, Mar. 2023. 2, 3

[12] S. Keil, *Technology and practical use of strain gages: with particular consideration of stress analysis using strain gages*. John Wiley & Sons, 2017. 2

[13] H. Liu, S. Guo, K. Zheng, X. Guo, T. Kuramoto-Ahuja, T. Sato, K. Onoda, and H. Maruyama, "Reliability and validity of measuring respiration movement using a wearable strain sensor in healthy subjects," *J. of Physical Therapy Science*, vol. 29, no. 9, pp. 1543–1547, 2017. 2

[14] A. L. Silva, M. Varanis, A. G. Mereles, C. Oliveira, and J. M. Balthazar, "A study of strain and deformation measurement using the Arduino microcontroller and strain gauges devices," *Revista Brasileira de Ensino de Física*, vol. 41, no. 3, Dec. 2018. 2, 3

[15] N. Lu, C. Lu, S. Yang, and J. Rogers, "Highly Sensitive Skin-Mountable Strain Gauges Based Entirely on Elastomers," *Advanced Functional Materials*, vol. 22, no. 19, pp. 4044–4050, Oct. 2012. 2

[16] S. Fallmann, R. Van Veen, L. Chen, D. Walker, F. Chen, and C. Pan, "Wearable accelerometer based extended sleep position recognition," in *IEEE Int. Conf. on e-Health Networking, Applications and Services (Healthcom)*. Dalian: IEEE, Oct. 2017, pp. 1–6. 2

[17] E. P. Doheny, M. M. Lowery, A. Russell, and S. Ryan, "Estimation of respiration rate and sleeping position using a wearable accelerometer," in *Int. Conf. of the IEEE Engineering in Medicine & Biology Society (EMBC)*. Montreal, QC, Canada: IEEE, Jul. 2020, pp. 4668–4671. 2

[18] F. J. Dian, A. Yousefi, and S. Lim, "A practical study on Bluetooth Low Energy (BLE) throughput," in *Information Technology, Electronics and Mobile Communication Conference (IEMCON)*. Vancouver, BC: IEEE, Nov. 2018, pp. 768–771. 2

[19] "Vernier Rasperatory Belt." [Online]. Available: https://www.vernier.com/product/go-direct-respiration-belt/?srsltid=AfmBOoqGIPv0diq6Yc_AdIHa079uciiYnNT6hpl9yBEVPQDCuMEvQYoC 3

[20] "Perfect Fit Rasperatory Belt." [Online]. Available: https://webshop.eegtech.com/en/accessoires-for-sleep/effort/perfect-fit-respiration-belt-pf-030-k.html 3

[21] "Natus Rasperatory Belt." [Online]. Available: https://natus.com/neuro/natus-xacttrace-rip-respiratory-effort-belts/ 3

[22] E. Schrüfer, L. M. Reindl, and B. Zagar, *Elektrische Messtechnik: Messung elektrischer und nichtelektrischer Größen*, 10th ed., ser. Hanser eLibrary. München: Hanser, 2012. 3

[23] M. Wrona, "Roll and Pitch Angles From Accelerometer Sensors," Dec. 2024. [Online]. Available: https://mwrona.com/posts/accel-roll-pitch/ 3

[24] Y. Tawil, "Towards understanding IMU: Basics of Accelerometer and Gyroscope Sensors and How to Compute Pitch, Roll and Yaw Angles," Mar. 2023. [Online]. Available: https://atadiat.com/en/e-towards-understanding-imu-basics-of-accelerometer-and-gyroscope-sensors/ 3

[25] A. Torres, E. Welsh, and A. Lammes, "Body Position Sensing with an Accelerometer/Gyroscope - Hackster.io." [Online]. Available: https://www.hackster.io/431666/body-position-sensing-with-an-accelerometer-gyroscope-5139e5 3

[26] M. Geiger, "Development of an inexpensive chest belt for measuring Respiratory Effort," Bachelor's Thesis, Graz University of Technology, Inffeldgasse 16/2, A-8010 Graz, Austria, Feb. 2025. 4

[27] M. S. A. A. S. Mahdi, "Investigating and Developing Low-Cost Wearable Respiration Sensors," Ph.D. dissertation, University of Southampton, Southampton, GB, Jun. 2023. [Online]. Available: https://eprints.soton.ac.uk/477832/1/PhD_Thesis_Final_Correction_PDFA_3b.pdf 5

[28] N. Hayward, M. Shaban, J. Badger, I. Jones, Y. Wei, D. Spencer, S. Isichei, M. Knight, J. Otto, G. Rayat, D. Levett, M. Grocott, H. Akerman, and N. White, "A capaciflector provides continuous and accurate respiratory rate monitoring for patients at rest and during exercise," *Journal of Clinical Monitoring and Computing*, vol. 36, no. 5, pp. 1535–1546, Oct. 2022. [Online]. Available: https://doi.org/10.1007/s10877-021-00798-7 5, 6

[29] R. Ross, W. M. Mongan, P. O'Neill, I. Rasheed, A. Fontecchio, G. Dion, and K. R. Dandekar, "An Adaptively Parameterized Algorithm Estimating Respiratory Rate from a Passive Wearable RFID Smart Garment," *Proceedings : Annual International Computer Software and Applications Conference. COMPSAC*, vol. 2021, pp. 774–784, Jul. 2021. [Online]. Available: https://pmc.ncbi.nlm.nih.gov/articles/PMC8463037/ 5, 6

[30] Binah.ai, "Respiratory Rate Accuracy Report (SDK 5.9.1)," Binah.ai, Technical Report. [Online]. Available: https://www.binah.ai/wp-content/uploads/2025/03/MED-000027-Respiratory-Rate-Accuracy-Report-of-SDK-5.9.1_Rev2-Final.pdf 5